

Influence of the magnetic field on the plasmonic properties of transparent Ni anti-dot arrays

Emil Melander,¹ Erik Östman,¹ Janine Keller,¹ Jan Schmidt,¹ Evangelos Th. Papaioannou,^{1,a)} Vassilios Kapaklis,¹ Unnar B. Arnalds,¹ B. Caballero,^{2,3} A. García-Martín,² J. C. Cuevas,³ and Björgvin Hjörvarsson¹

¹Department of Physics and Astronomy, Uppsala University, Box 516, SE-751 20 Uppsala, Sweden

²IMM-Instituto de Microelectrónica de Madrid (CNM-CSIC), Isaac Newton 8, PTM, Tres Cantos, E-28760 Madrid, Spain

³Departamento de Física Teórica de la Materia Condensada, Universidad Autónoma de Madrid, 28049 Madrid, Spain

(Received 20 May 2012; accepted 24 July 2012; published online 7 August 2012)

Extraordinary optical transmission is observed due to the excitation of surface plasmon polaritons in 2-dimensional hexagonal anti-dot patterns of pure Ni thin films, grown on sapphire substrates. A strong enhancement of the polar Kerr rotation is recorded at the surface plasmon related transmission maximum. Angular resolved reflectivity measurements under an applied field reveal an enhancement and a shift of the normalized reflectivity difference upon reversal of the magnetic saturation (transverse magneto-optical Kerr effect-TMOKE). The change of the TMOKE signal clearly shows the magnetic field modulation of the dispersion relation of SPPs launched in a 2D patterned ferromagnetic Ni film. © 2012 American Institute of Physics. [<http://dx.doi.org/10.1063/1.4742931>]

Magneto-plasmonics offer unique possibilities to manipulate light by the use of external magnetic fields.^{1–4} The prevailing choice of materials for fabrication of magneto-plasmonic structures has been combined structures of noble and magnetic metals/dielectrics, such as Au and Co/Iron garnet.^{1,5,6} The basic idea behind this choice is the combination of the large plasmon activity of noble metals with the magnetic functionality provided by the additional materials. Another reason for the use of noble metals is the excellent resistance to oxidation, which is required to obtain durable patterned thin films. Ni is an interesting candidate in this context as it forms a thin and self-passivating oxide layer (approximately 1 nm).^{7,8} Furthermore, the magneto-optical activity of Ni-based nano-patterns can be enhanced by the presence of surface plasmon polaritons (SPPs).^{9–13}

The magnetic field can provide the means for control of SPPs, as it has been predicted for noble metals,¹⁴ and explored experimentally in hybrid structures.^{2,5,6} Early studies on this effect were targeted towards semiconductor-based SPPs (Ref. 15) but not in metallic systems, where high magnetic fields are required.¹⁶ In pure magnetic materials, the need for high fields is not present as the magneto-optical effects are sufficiently strong.

In this Letter, we discuss the influence of an external magnetic field on the SPPs for the case of a pure magnetic metal, such as Ni, patterned in two-dimensions (2D) on a transparent substrate. We examine to what extent the ferromagnetic Ni can be used as a host material for SPPs. We show that the magnetic field induces a modulation of the dispersion of SPPs excitation in Ni.

A Ni anti-dot sample was prepared on a double side polished Al₂O₃ [1120] substrate. The patterning was accomplished by the use of self-organization of colloidal

polystyrene beads as shadow masks.⁹ A 30 nm thick Ni film was deposited on the masked sapphire substrate, using electron-beam evaporation. A snapshot of the procedure is illustrated in Fig. 1, where both the shadow mask and the resulting holes are clearly seen. This process resulted in a well defined Ni layer, decorated by holes of a diameter $d = 300$ nm, spaced on an hexagonal lattice of periodicity of $a = 450$ nm. The ratio of the radius to pitch size was determined to be $\pi d^2 / (2\sqrt{3}a^2) = 0.40$, leaving a total surface for the Ni film of 60%, with respect to the substrate area.

Magneto-optic spectra were recorded using a magneto-optic Kerr spectrometer operating in the polar configuration with an angle of incidence of 4° and a maximum applied magnetic field of 1.7 T. The range in recorded wavelength is 250–1000 nm. Angular dependent zero-order reflectivity curves ($\theta - 2\theta$) were obtained using a dedicated optical diffractometer (HUBER MC 9300), with a step resolution of

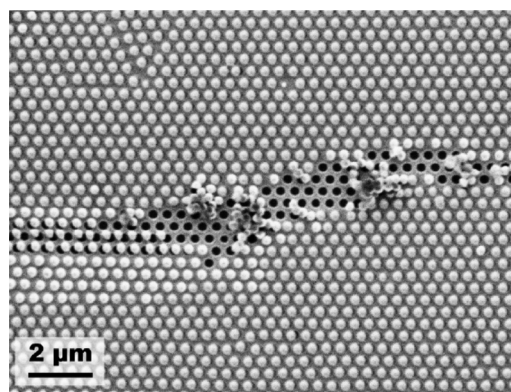


FIG. 1. Scanning electron microscopy image of the sample surface after evaporation of Ni. The image depicts the stage of the lift off of the self-assembled polystyrene beads, which leaves behind an antidot patterned film of Ni. The resulting sample has an average pitch size of $a = 450$ nm and hole diameter of $d = 300$ nm.

^{a)} Author to whom correspondence should be addressed. Electronic mail: vangelis@physics.uu.se.

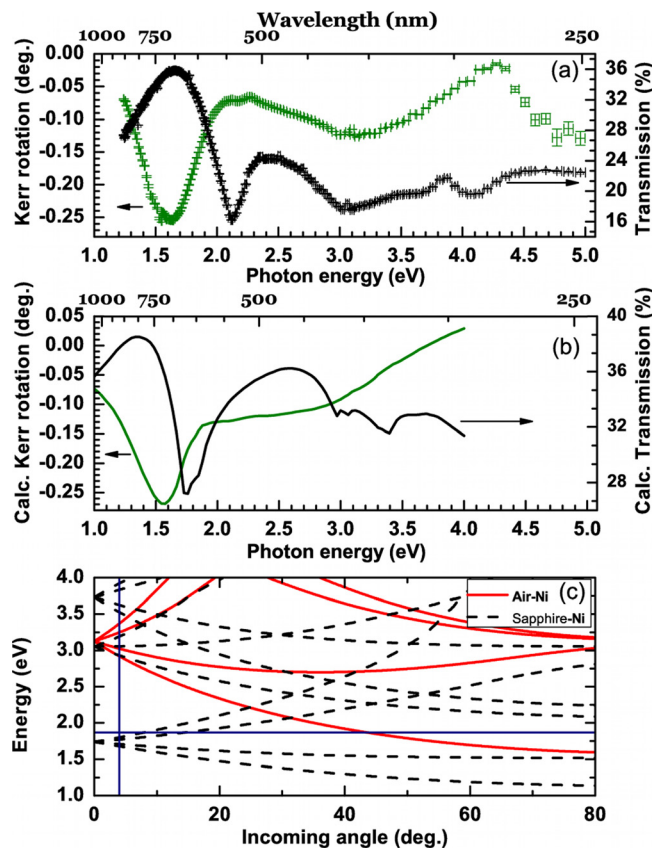


FIG. 2. (a) Experimental transmission and polar Kerr rotation spectra for the Ni antidot structure of Fig. 1. Kerr values were obtained with the film at the saturated state ($B = 1.7$ T). The transmission curve has been corrected for the substrate. (b) Calculated transmission and polar Kerr rotation spectra. (c) Calculated dispersion relation of the Bragg plasmons both for the Ni/air interface and Ni/sapphire interface. The vertical line is drawn at 4° and the horizontal line at 660 nm.

$1/1000^\circ$ and a laser wavelength of $\lambda = 660$ nm.⁹ A magnetic field up to 42 mT can be applied, using a quadrupole air core coil magnet, which is mounted on the sample rotation stage of the goniometer.

Fig. 2(a) shows the experimental and (b) the calculated transmission and polar Kerr rotation spectra for the sample. The calculations have been made using the scattering formalism described in Ref. 17, using the optical and magneto-optical elements of the dielectric tensor given in Ref. 18, extended with those of Ref. 19 to include energies below 1.5 eV.

The experimental transmission curve in Fig. 2(a) exhibit several maxima. The calculated one in Fig. 2(b) shows a similar shape like in the experiment. If SPP modes are involved, then the energies at which the maxima appear must be close to the energies corresponding to the so called Bragg plasmons (SPPs modes coupled to the lattice periodicity). The calculated dispersion relation of those Bragg plasmons is presented in Fig. 2(c) finding a fair match for the transmission maxima. As we move to higher frequencies, the absorption plays more and more a significant role and that implies a shift and a widening of the resonance peaks. In addition as we can see from Fig. 2(c), at higher frequencies, modes from the upper and lower interface begin to mix resulting in an overlapping of different resonances. Additional calculations (not shown) revealed that the coupling between the so-called

low-index and the high-index plasmons at each interface is negligible.

The overlap of the overall transmission maxima and the enhancement of the Kerr rotation, further prove the existence of SPPs in the sample.^{3,4,9} The first peak in transmission records an intensity of $\sim 36\%$ (after substrate corrections). Although it is expected the plasmon losses in Ni to be large, we have a clear indication of a strong SPP resonance. The propagation length of SPPs in Ni at 1.6 eV (Ref. 20) is calculated to be 840 nm and decreases strongly with increasing energy, resulting in low transmission values as in Fig. 2(a). Transmission minima are related to so-called Wood-Rayleigh anomalies.²¹ In a good metal, the spectral location of the Wood-Rayleigh anomaly is close to the condition for SPPs excitation on a metal-dielectric interface. In our case, plasmon excitation occurs at slightly smaller energies (larger wavelengths) than the appearance of a diffracted beam. As a result, maxima and minima are close to each other.

Angular resolved reflectivity measurements are also a way to explore the effect of SPPs in anti-dot structures.⁹ In Fig. 3(a) (left y-axis), we present angular reflectivity measurements at a wavelength of $\lambda = 660$ nm for p-polarized light. This corresponds to the region in between the first transmission maximum in Fig. 2(a) and the transmission minimum, or in other words around a region with a large variation of transmission, $T(\lambda)$. The data were obtained having the hexagonal pattern aligned with one of its major symmetry axes (ΓK) parallel to the scattering plane. The trough in reflectivity at 42° is a signature of surface plasmons excitations. The minimum in reflectivity is close to the theoretical

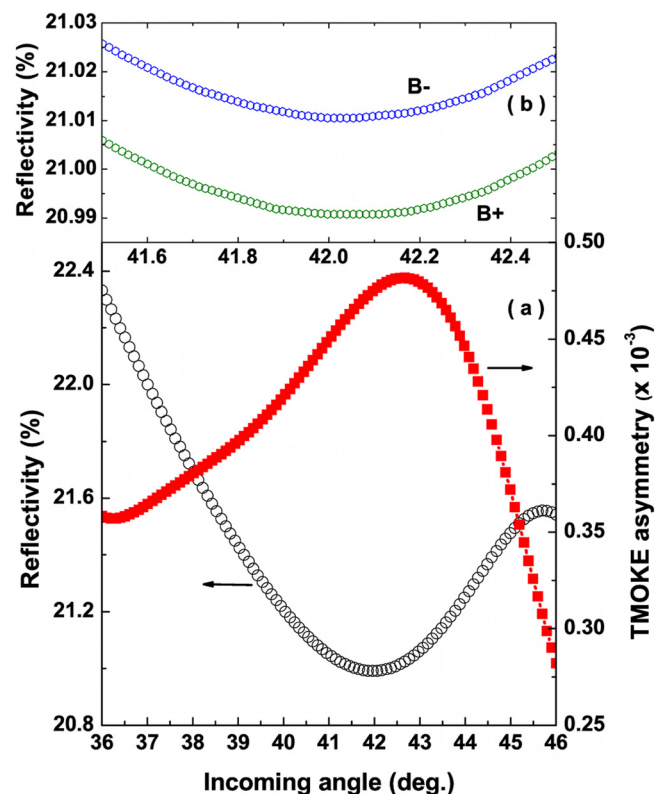


FIG. 3. (a) Reflectivity (black dot-line, left axis) and the TMOKE (red square-line, right axis). The TMOKE signal presents a clear shift and enhancement. (b) Reflectivity in the angular range of the minimum in the ΓK direction for the two directions of the magnetization.

value for the Bragg plasmon at that specific frequency (~ 1.85 eV), as shown by the horizontal line in Fig. 2(c). The width of the reflection minimum is broader than those for noble metals due to the higher absorption losses of Ni. There is an additional broadening due to the ratio of the hole depth (30 nm) to the hole diameter (300 nm). If the ratio is close to unity, the features are sharper than for lower ratios.²¹

In order to investigate any influence of the magnetic field on the SPPs resonances, the transverse magneto-optic Kerr effect (TMOKE) can be a very useful tool. The orientation of the magnetic field with respect to the SPPs propagation direction and the light polarization is of key importance^{2,5} defining the magnitude of the magnetic field—SPPs interaction. TMOKE is defined as the magnetization modulated intensity difference of the reflected light

$$\text{TMOKE} = \frac{R(M+) - R(M-)}{R(M+) + R(M-)} \quad (1)$$

The applied magnetic field lies in the plane of the film and perpendicular to the plane of incidence (and in our case, also perpendicular to the SPPs propagation along the ΓK direction). In this configuration, the magnetic field influences only the optical reflectivity. The size of the applied magnetic field was 20 mT, enough for the magnetic saturation of the sample. Worth noticing is that the magnetization of the Ni nano-patterned film lies in the film plane (saturation field of 14 mT for the transverse case) while a high field of 0.45 T is needed to saturate the sample out of plane.

The application of a transverse field induces a small change in the position of the minimum and the width of the resonant position of the SPPs, and a variation of the intensity of the overall reflectivity (see Fig. 3(b)). In the case of a ferromagnetic dielectric film^{2,22} or Co layer⁵ covered by a thin smooth/or perforated noble metal, a transverse applied field shifts the plasmon related reflectivity (transmission) minimum (maximum) and an enhanced TMOKE appears. A similar behavior is observed here in the Ni film, having a 2D nano-pattern without the support of a noble metal. The TMOKE signal presented as a red square-line in Fig. 3(a) appears shifted with regards to the reflectivity minimum and enhanced compared to the featureless TMOKE (not shown) response of a 30 nm thick continuous reference Ni film. The enhancement can be attributed to the proximity of the used wavelength ($\lambda = 660$ nm) to the SPPs resonances at the metal/air interface (see Fig. 2(b)). TMOKE is featureless when measured away from the excitation region. We can understand this behavior if we consider that TMOKE can be approximated as the product of two terms:¹⁶ one is the frequency derivative of the reflection (transmission) spectrum and the other is the magnetic field induced frequency shift. Hence, TMOKE is expected to be enhanced near the SPPs resonant wavelength even for the case of smooth interface as it has been observed in continuous thin films of Ni in early works.²³

To get further insight, we have performed numerical simulations of the reflectivity and of the TMOKE signal, using a recently developed formalism that uses the scattering matrix approach adapted to deal with arbitrary orientations

of the magnetization,²⁴ using the same elements for the dielectric tensor as for the Polar Kerr effect. The simulated results depicted in Fig. 4(a) are in very good agreement with the experimental findings. Moreover, in Fig. 4(b), we show the evolution of the reflectivity minimum and the TMOKE maximum as a function of the in-plane angle. As one can see, the position of these two features follows nicely the dispersion relation of the relevant Bragg plasmon, which is shown as a dashed line in both panels. This clearly shows that the plasmon excitation is responsible for these two features. Furthermore, Fig. 4(b) shows that outside the excitation region, the reflectivity and TMOKE signals are featureless and the system behaves as an uniform medium made of a mixture of Ni and air.

In summary, we have shown that a Ni thin film patterned in a 2D hexagonal antidot array supports the excitation of SPPs both at the air/Ni interface and Ni/substrate interface. Transmission and reflection measurements reveal the excitation of SPPs with broader resonances due to the high damping of SPPs in ferromagnets. The dispersion relation of SPPs defined by the hexagonal pattern can be modified with an application of a transverse magnetic field as the TMOKE modulated reflectivity signal reveals. The enhancement and the shift of the TMOKE curve is significant and can be altered by the incoming wavelength and angle of incidence.

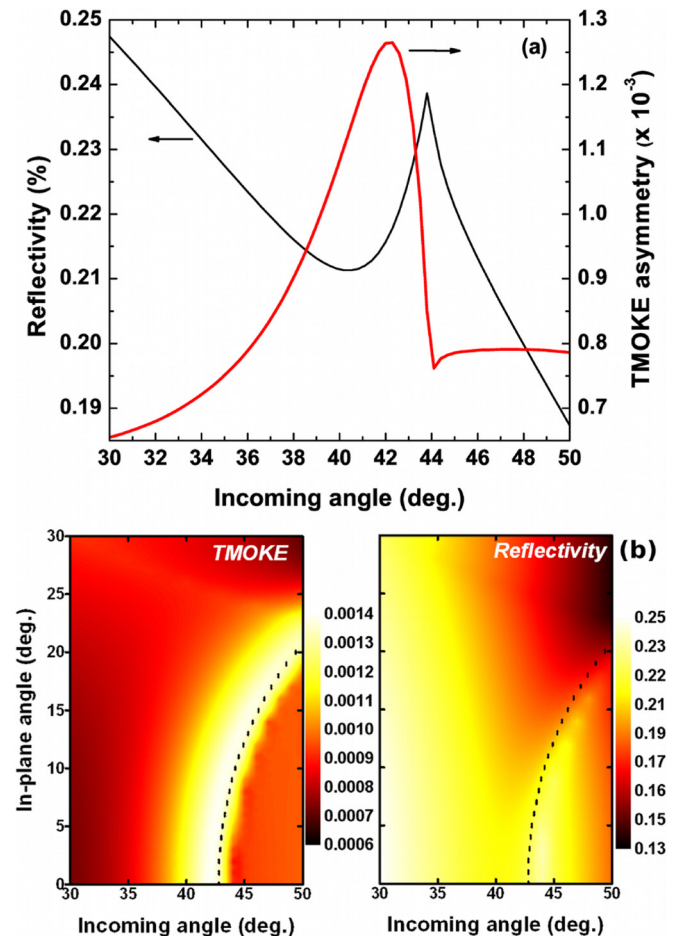


FIG. 4. (a) Calculated reflectivity in the angular range of the minimum in the ΓK direction (black line, left axis) and the TMOKE (red line, right axis). (b) Calculated reflectivity (right panel) and TMOKE (left panel) in the same angular range as in (a) along different in-plane directions, going from the ΓK (0°) to the ΓM (30°) along the KM direction.

These effects pave the road for the development of new optical components and sensors with great application potential.

The authors would like to thank Piotr Patoka for the preparation of the polystyrene bead template. The authors acknowledge the support of the Swedish Research Council (VR), the Knut and Alice Wallenberg Foundation (KAW), and the Swedish Foundation for International Cooperation in Research and Higher Education (STINT). B.C. and A.G.-M. acknowledge funding from the EU (NMP3-SL-2008-214107-Nanomagma), the Spanish MICINN (“MAPS” MAT2011-29194-C02-01, and “FUNCOAT” CONSOLIDER INGENIO 2010 CSD2008-00023), and the Comunidad de Madrid (“MICROSERES-CM” S2009/TIC-1476). J.C.C. acknowledges financial support from the Spanish MICINN (Contract No. FIS2011-28851-C02-01).

- ¹V. V. Temnov, G. Armelles, U. Woggon, D. Guzatov, A. Cebollada, A. Garcia-Martin, J.-M. Garcia-Martin, T. Thomay, A. Leitenstorfer, and R. Bratschitsch, *Nature Photon.* **4**, 107 (2010).
- ²V. I. Belotelov, I. A. Akimov, M. Pohl, V. A. Kotov, S. Kature, A. S. Vengurlekar, G. A. Venu, D. R. Yakovlev, A. K. Zvezdin, and M. Bayer, *Nat. Nanotechnol.* **6**, 370 (2011).
- ³G. Ctistis, E. Papaioannou, P. Patoka, J. Gutek, P. Fumagalli, and M. Giersig, *Nano Lett.* **9**, 1 (2009).
- ⁴E. T. Papaioannou, V. Kapaklis, P. Patoka, M. Giersig, P. Fumagalli, A. Garcia-Martin, E. Ferreiro-Vila, and G. Ctistis, *Phys. Rev. B* **81**, 054424 (2010).
- ⁵D. Martin-Becerra, J. B. Gonzalez-Diaz, V. V. Temnov, A. Cebollada, G. Armelles, T. Thomay, A. Leitenstorfer, R. Bratschitsch, A. Garcia-Martin, and M. U. Gonzalez, *Appl. Phys. Lett.* **97**, 183114 (2010).
- ⁶G. A. Wurtz, W. Hendren, R. Pollard, R. Atkinson, L. L. Guyader, A. Kirilyuk, T. Rasing, I. I. Smolyaninov, and A. V. Zayats, *New J. Phys.* **10**, 105012 (2008).

- ⁷P. Pouloupoulos, V. Kapaklis, P. E. Jonsson, E. T. Papaioannou, A. Delimitis, S. D. Pappas, D. Trachylis, and C. Politis, *Appl. Phys. Lett.* **96**, 202503 (2010).
- ⁸R. Saiki, A. Kaduwela, M. Sagurton, J. Osterwalder, D. Friedman, C. Fadley, and C. Brundle, *Surf. Sci.* **282**, 33 (1993).
- ⁹E. T. Papaioannou, V. Kapaklis, E. Melander, B. Hjörvarsson, S. D. Pappas, P. Patoka, M. Giersig, P. Fumagalli, A. Garcia-Martin, and G. Ctistis, *Opt. Express* **19**, 23867 (2011).
- ¹⁰V. Bonanni, S. Bonetti, T. Pakizeh, Z. Pirzadeh, J. Chen, J. Nogués, P. Vavassori, R. Hillenbrand, J. Åkerman, and A. Dmitriev, *Nano Lett.* **11**, 5333 (2011).
- ¹¹J. Chen, P. Albella, Z. Pirzadeh, P. Alonso-González, F. Huth, S. Bonetti, V. Bonanni, J. Åkerman, J. Nogués, P. Vavassori, A. Dmitriev, J. Aizpurua, and R. Hillenbrand, *Small* **7**, 2341 (2011).
- ¹²A. A. Grunin, A. G. Zhdanov, A. A. Ezhov, E. A. Ganshina, and A. A. Fedyanin, *Appl. Phys. Lett.* **97**, 261908 (2010).
- ¹³J. F. Torrado, J. B. Gonzalez-Diaz, G. Armelles, A. Garcia-Martin, A. Altube, M. Lopez-Garcia, J. F. Galisteo-Lopez, A. Blanco, and C. Lopez, *Appl. Phys. Lett.* **99**, 193109 (2011).
- ¹⁴Y. M. Strel'niker and D. J. Bergman, *Phys. Rev. B* **77**, 205113 (2008).
- ¹⁵A. Hartstein and E. Burstein, *Solid State Commun.* **14**, 1223 (1974).
- ¹⁶J. B. González-Díaz, A. García-Martín, G. Armelles, J. M. García-Martín, C. Clavero, A. Cebollada, R. A. Lukaszew, J. R. Skuza, D. P. Kumah, and R. Clarke, *Phys. Rev. B* **76**, 153402 (2007).
- ¹⁷A. Garcia-Martin, G. Armelles, and S. Pereira, *Phys. Rev. B* **71**, 205116 (2005).
- ¹⁸S. Visnovsky, V. Parizek, M. Nyvlt, P. Kielar, V. Prosser, and R. Krishman, *J. Magn. Magn. Mater.* **127**, 135 (1993).
- ¹⁹K. Mok, C. Scarlat, G. J. Kovács, L. Li, V. Zviagin, J. McCord, M. Helm, and H. Schmidt, *J. Appl. Phys.* **110**, 123110 (2011).
- ²⁰Palik, *Handbook of Optical Constants of Solids Part II*, edited by E. D. Palik (Academic, New York, 1985).
- ²¹T. W. Ebbesen, H. J. Lezec, H. F. Ghaemi, T. Thio, and P. A. Wolff, *Nature (London)* **391**, 667 (1998).
- ²²V. I. Belotelov, D. A. Bykov, L. L. Doskolovich, A. N. Kalish, and A. K. Zvezdin, *J. Opt. Soc. Am. B* **26**, 1594 (2009).
- ²³P. Ferguson, O. Stafsudd, and R. Wallis, *Physica B & C* **89**, 91 (1977).
- ²⁴B. Caballero, A. García-Martín, and J. C. Cuevas, *Phys. Rev. B* **85**, 245103 (2012).